

AoI-Aware Co-Design of Cooperative Transmission and State Estimation for Marine IoT Systems

Ling Lyu^{ID}, *Member, IEEE*, Yanpeng Dai^{ID}, *Member, IEEE*, Nan Cheng, *Member, IEEE*,
Shanying Zhu^{ID}, *Member, IEEE*, Xiping Guan^{ID}, *Fellow, IEEE*, Bin Lin^{ID}, *Member, IEEE*,
and Xuemin Shen^{ID}, *Fellow, IEEE*

Abstract—In smart ocean, unmanned surface vehicles (USVs) are deployed to monitor the marine environment in a coordinated manner. The ubiquitous situation awareness of marine environment can be achieved by state estimation with the sensory data collected by USVs. Therefore, the transmission performance in terms of packet loss and delay of sensory data plays an important role in the state estimation of marine IoT systems. However, it is challenging to achieve the high-reliable and low-latency transmission for sensory data due to the path loss, spectrum scarcity and transmit power limitation. In this article, we introduce the Age of Information (AoI) to mathematically characterize the impacts of packet loss and transmission delay on the state estimation error. We first explore the relationship between the state estimation error and the AoI of sensory data. We then investigate the co-design of state estimation and sensory data transmission for marine IoT systems. Specifically, a mother ship (MS)-assisted cooperative transmission scheme is proposed to mitigate the impact of limited resources and path loss on the estimation performance. Then, the MS location, channel allocation, and transmit power are jointly optimized to minimize

the mean-square error of state estimation, which is achieved by formulating a constrained minimization problem and solving it with the decomposition method. Simulation results demonstrate that the proposed scheme has superiorities in reducing the estimation error and the power consumption.

Index Terms—Age of Information (AoI), cooperative transmission, marine Internet of Things (IoT) systems, state estimation.

I. INTRODUCTION

WITH the rapid deployment of wireless communication technologies, the emerging Internet-of-Things (IoT) system has a wide range of applications in smart ocean, such as marine environment monitoring, offshore exploration, and maritime search and rescue [1]–[5]. Recently, unmanned surface vehicles (USVs) have attracted many attentions from both the industry and academia, due to the advantages of on-demand deployment and flexible network architecture [6]. Take the marine environment monitoring for example, where multiple USVs cooperatively monitor the environment state and transmit the sensory data via wireless channels to the onshore base station (OBS). The OBS estimates the state of the marine environment based on the received sensory data [7]. However, USV-based marine IoT systems suffer from some practical constraints, such as limited transmit power, limited sensing range, and limited spectrum resource. These constraints restrict the wireless transmission performance, i.e., increasing packet loss and prolonging transmission delay [8]–[12]. If the OBS cannot successfully receive the sensory data within the prescribed deadline, it has to conjecture the current state based on previous sensory data, which enlarges the estimation error and deteriorates the monitoring performance. Therefore, it is crucial to provide the high-reliable and low-latency data transmission for the monitoring performance in marine IoT systems.

As the estimation error depends on the transmission performance of sensory data, many related works have paid attentions on how to minimize the mean-square error (MSE) under the constraints of packets loss and transmission delay [13]. Rana *et al.* [14] investigated the interconnected optimal filtering problem for distributed dynamic state estimation considering measurement losses caused by unreliable wireless communications. On this basis, the problem of the distributed federated Kalman filter fusion for a class of multisensor unreliable networked systems is studied in [15]. Moreover, due to the limited battery capacity of sensors,

Manuscript received July 20, 2020; revised October 26, 2020; accepted November 23, 2020. Date of publication November 30, 2020; date of current version May 7, 2021. This work was supported in part by the National Natural Science Foundation of China under Grant 62002042, Grant 62071356, Grant 61922058, Grant 61971083, Grant 51939001, Grant 62025305, and Grant 61933009; in part by the National Key Research and Development Program of China under Grant 2019YFE0111600; in part by the Program of Shanghai Academic Research Leader under Grant 19XD1421800; in part by the National Natural Science Foundation of Shanghai Municipality of China under Grant 18ZR1419900; in part by the Cooperative Scientific Research Project, Chunhui Program of Ministry of Education, China; and in part by the Dalian Science and Technology Innovation Fund under Grant 2019J11CY015. (Corresponding author: Yanpeng Dai.)

Ling Lyu is with School of Information Science and Technology, Dalian Maritime University, Dalian 116026, China, also with the State Key Laboratory of Integrated Services Networks, Xidian University, Xi'an 710071, China, and also with the Key Laboratory of System Control and Information Processing, Ministry of Education of China, Shanghai 200240, China (e-mail: linglyu@dlmu.edu.cn).

Yanpeng Dai is with the School of Information Science and Technology, Dalian Maritime University, Dalian 116026, China (e-mail: yanpengdai@dlmu.edu.cn).

Nan Cheng is with the School of Telecommunication Engineering, Xidian University, Xi'an 710071, China (e-mail: nancheng@xidian.edu.cn).

Shanying Zhu and Xiping Guan are with the Department of Automation and the Key Laboratory of System Control and Information Processing, Ministry of Education of China, Shanghai Jiao Tong University, Shanghai 200240, China (e-mail: shyzhu@sjtu.edu.cn; xpguan@sjtu.edu.cn).

Bin Lin is with the School of Information Science and Technology, Dalian Maritime University, Dalian 116026, China, and also with the Network Communication Research Center, Peng Cheng Laboratory, Shenzhen 518052, China (e-mail: binlin@dlmu.edu.cn).

Xuemin Shen is with the Department of Electrical and Computer Engineering, University of Waterloo, Waterloo, ON N2L 3G1, Canada (e-mail: sshen@uwaterloo.ca).

Digital Object Identifier 10.1109/IIOT.2020.3041287

Ren *et al.* [16] jointly designed the transmit power control rule and the remote estimation scheme to guarantee the estimation performance with minimized energy consumption. The aforementioned works mainly focus on the optimization of state estimation to alleviate the adverse impact of harsh wireless environments and limited energy resource on the transmission reliability and latency, which could be regarded as a passive manner to tolerate the packets loss and transmission delay. In fact, this passive manner may restrict the improvement of estimation performance, since the path loss and the limited transmit power make the received signal strength not sufficiently large to be decoded successfully.

From the perspective of wireless transmission, many works have investigated how to achieve the high-reliable and low-latency transmission in a proactive manner. Cooperative transmission [17] could improve the transmission reliability by taking advantage of the spatial diversity gain to enhance the received signal strength and spectrum utilization. The performance of a series of cooperative transmission schemes are compared in terms of maximum outage probability and end-to-end throughput [18]. Considering the energy limitation, Hiraguri *et al.* [19] proposed a cooperative retransmission control scheme to achieve high reliability and transmission efficiency. On this basis, Shi *et al.* [20] investigated a cooperative transmission scheme to maximize average throughput and spectral efficiency by jointing designing the interference-aware rate selection and power allocation. Moreover, for the system control over shared wireless channels, Lyu *et al.* [21] proposed a hybrid-mode cooperative transmission scheme to provide the required transmission reliability for wireless control systems. Due to the advantages of high diversity gain and spectrum utilization, cooperative transmission is employed in this article to proactively provide a reliable data transmission for the state estimation in marine IoT systems. However, the aforementioned works could not be directly applied to the data transmission in marine IoT systems, since the mother-ship (MS) mobility makes the cooperation scheme and the location optimization tightly coupled.

In order to incorporate the effect of packet loss and transmission delay on the state estimation, Age of Information (AoI) is introduced [22]. AoI is regarded as an emerging performance metric to measure the timeliness and freshness of state information available at the destination [23], thus it is quite suitable for IoT applications with time-sensitive and high-reliable data. Due to random characteristics of wireless channels, the average AoI is generally used to describe the integrated effect of packet loss and transmission delay on the sensory data [24]. Recently, a great deal of works have focused on minimizing average AoI for machine-type applications [25]. Wang *et al.* [26] optimized the average AoI under the constraints of available spectrum and energy resources. Moreover, Kadota *et al.* [27] investigated the scheduling algorithm for a number of nodes to minimize the expected weighted sum of AoI within the budget of energy consumption. Wang *et al.* [28] and Zhou *et al.* [29] investigated the energy-efficient heterogeneous network association and resource allocation under the stringent quality of service requirements. Abdel-Aziz *et al.* [30] studied the transmission power minimization problem under constraints

of probabilistic AoI for both deterministic and Markovian traffic arrivals. Moreover, this work analyzes the tradeoff between average AoI and total average transmitted power in simulation. From this result, it can be seen that the total average transmitted power decreases with the increasing of average AoI. Inspired by the superiorities of average AoI in characterizing the impact of packets loss and transmission delay on the IoT applications, we aim to integrate the metric of average AoI into the performance evaluation of state estimation in marine IoT systems. In order to achieve the aim, it is essential to explore the relationship between estimation performance and average AoI.

In this article, we investigate the co-design of state estimation and sensory data transmission for marine IoT systems. We first present a two-hop cooperative transmission architecture, where the MS relays the sensory data of USVs to the OBS for estimating the state of the marine environment. Under this architecture, the average AoI of sensory data is adopted to characterize the impact of packets loss and transmission delay on the MSE of state estimation. On this basis, we design an MS-assisted cooperative transmission scheme, which jointly optimizes the MS location, channel allocation, and transmit power to minimize the average AoI for state estimation. The contributions of this article are summarized as follows.

- 1) We mathematically characterize the effect of packet loss and transmission delay on the average AoI of sensory data, which makes it possible to design an effective AoI-penalty-aware state estimation for marine IoT systems.
- 2) We explore that the MSE of state estimation increases exponentially with the growth of the average AoI of sensory data. Based on this exploration, an MS-assisted cooperative transmission scheme is proposed to minimize the MSE of state estimation.
- 3) The proposed scheme effectively reduces state estimation error and power consumption for environment monitoring in marine IoT systems. Specially, many-to-one matching theory and Karush–Kuhn–Tucker (KKT) conditions are adopted to optimize MS location and USV-MS association in an iterative manner. Moreover, a heuristic channel allocation algorithm and a water filling-based power allocation algorithm are designed to minimize the average AoI of sensory data.

The remainder of this article is organized as follows. The system model is presented in Section II. Section III presents the cooperative transmission design for AoI-penalty-aware state estimation. In Section IV, the MS location, channel allocation, and transmit power are jointly optimized to improve the transmission performance and reduce the estimation error for marine IoT systems. Simulation results and main conclusions are shown in Sections V and VI, respectively.

II. SYSTEM MODELS

The considered marine IoT system is shown in Fig. 1. Multiple USVs are deployed on the sea surface to collect the sensory data of the marine environment in a coordinated manner. USVs deliver the sensory data to one MS over assigned channels, and MS forwards the received data to OBS (see

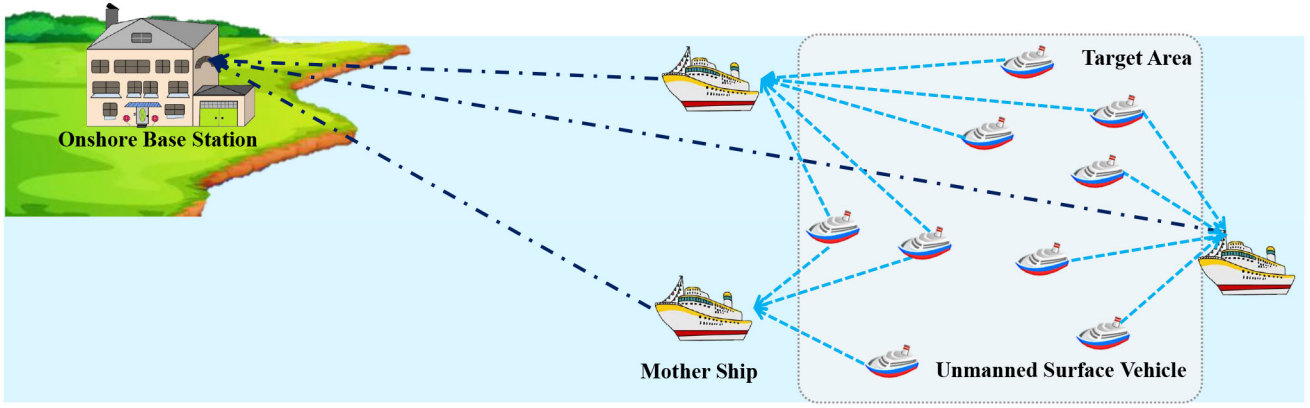


Fig. 1. USV-based marine IoT system.

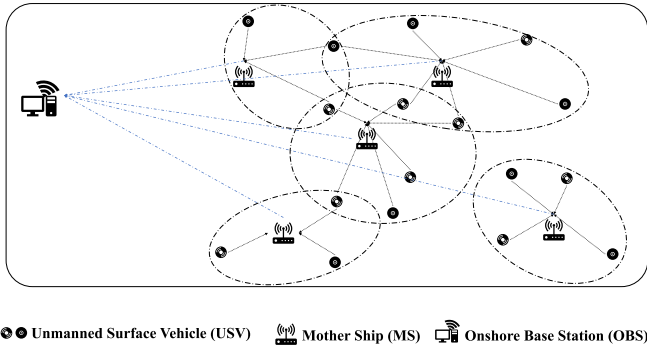


Fig. 2. Network architecture for the considered marine IoT system.

Fig. 2). MSs work in the out band full-duplex mode acting as the relay in cooperative transmission. Based on the received sensory data, the OBS performs the state estimation to monitor the marine environment. As a result, the performance of state estimation is restricted by the transmission rate in the USV-MS and MS-OBS transmission stages, which is determined by the MSs' location, USV association, channel allocation, and transmit power.

A. System Model

The state of the considered marine environment evolves over time based on the following discrete time dynamics [31]:

$$\mathbf{x}_n(t+1) = \mathbf{A}\mathbf{x}_n(t) + \mathbf{v}_n(t) \quad (1)$$

where $\mathbf{x}_n(t)$ is the system state obtained by the n th USV at the time step t , the system noise $\mathbf{v}_n(t)$ is Gaussian with zero mean and covariance matrices $\mathbf{Q}_n > 0$, and \mathbf{A} denotes the system matrix. Without loss of generality, we assume that the control system is controllable but unstable, i.e., $\rho(\mathbf{A}) > 1$ and the control pair is stabilized,¹ where $\rho(\cdot)$ is the spectral radius of a matrix. The initial state $\mathbf{x}_n(0)$ is a Gaussian random vector with the mean $\bar{\mathbf{x}}_n(0)$ and covariance matrix $\mathbf{W}_n(0)$.

¹If the system (1) is stable, the analysis, designed scheme, and optimization method given in this article are still applicable.

B. Communication Model

The considered cooperative transmission system includes N USVs, S MSs, and one OBS. In practice, USVs performing different monitoring missions are equipped with different types of sensors. Let $l_n(t)$ denote the length of data packet generated by the n th USV at the t th time step. Moreover, if the n th USV is associated to the s th MS at the t th time step, the binary variable $\delta_{s,n}(t) = 1$. Otherwise, $\delta_{s,n}(t) = 0$. Each USV can be associated to only one MS, i.e., $\sum_{s=1}^S \delta_{s,n}(t) = 1$. The set of USVs associated to the s th MS is denoted by $\mathcal{N}_s(t) = \{n | \delta_{s,n}(t) = 1\}$, whose cardinality is $N_s(t)$.

The available bandwidth is evenly split to K independent wireless channels, and the bandwidth of each channel is B . Let the binary variable $\theta_{n,k}(t)$ denote that whether the channel k is assigned to the n th USV at the t th time step. If so, $\theta_{n,k}(t) = 1$; otherwise, $\theta_{n,k}(t) = 0$. For simplicity, the integration of s th MS and its associated USVs $\mathcal{N}_s(t)$ is denoted by the s th group $\mathcal{M}_s(t)$. Let $\mathbf{k}_s(t) = \{k | \delta_{s,n}(t) = 1, \theta_{n,k}(t) = 1 \forall n \in \mathcal{N}_s(t) \forall k \in \mathcal{K}\}$ denote the set of channels allocated for all devices in the s th group, and $\|\mathbf{k}_s(t)\|_1 = K_s(t)$ and $\sum_{s=1}^S K_s(t) \leq K$.

III. COOPERATIVE TRANSMISSION DESIGN FOR AOI-PENALTY-AWARE STATE ESTIMATION

A. Location-Dependent Two-Hop Data Rate

The most important and distinctive characteristics of maritime wireless channels are the location-dependent property. The horizontal location of MS and USV is denoted by $\mathbf{z}_s(t) = [a_s(t), b_s(t)]$ and $\mathbf{z}_n(t) = [a_n(t), b_n(t)]$ by assuming that altitude intercepts among devices are negligible [32]. The path loss of wireless transmission between the n th USV and the s th MS is by $d_{s,n}(t) = \sqrt{(a_n(t) - a_s(t))^2 + (b_n(t) - b_s(t))^2}$. The horizontal location of each MS can be optimized, and each USV is fixed in the monitoring area. According to [33], the wireless channel between MSs and USVs experiences heavy reflection from sea surface, resulting in the severe multipath effects. For notation simplify, the channel power gain of the k th wireless channel between the n th USV and the s th MS is denoted as $g_{s,n,k_{um}}(t)$. On the contrary, the dominant path loss of wireless channel between the OBS and MSs can be considered as the light-of-sight path. The channel power gain of the k th wireless channel between the s th MS

and OBS is denoted as $g_{s,kmo}(t)$. For the offshore USV-MS transmission stage, the Rayleigh fading is adopted to characterize the reflection from the sea surface, which is given by $g_{s,n,kum}(t) = [(G_{s,nrx}G_{s,nrx}\varsigma)/(16\pi^2(d_{s,n}(t)/d_0)^2)] \cdot h_{s,n,kum}$, where $d_{s,n}(t)$ is the transmission distance, d_0 is a far field reference distance, ς is carrier wavelength, and the small-scale fading $h_{s,n,kum}^{um}$ is Rayleigh distributed. Furthermore, the Rician fading is adopted to characterize the wireless channel for the near-shore MS-OBS transmission [34], which is given by $g_{s,kmo}(t) = [(G_{s,0rx}G_{s,0rx}\varsigma)/(16\pi^2(d_{s,0}(t)/d_0)^2)] \cdot h_{s,k}^{mo}$, where $h_{s,k}^{mo}$ obeys the Rician distribution, and $d_{s,0}(t) = \sqrt{(a_s(t) - a_0(t))^2 + (b_s(t) - b_0(t))^2}$ is the transmission distance between the s th MS and OBS.

The achievable data rate between the n th USV and the s th MS is expressed as

$$R_{s,n,kum}(t) = B \log_2 \left(1 + \sum_{k=1}^K \theta_{n,k}(t) p_{n,k}(t) \gamma_{s,n,kum}(t) \right) \quad (2)$$

where $p_{n,k}(t)$ is the transmit power of the n th USV on the k th channel. $\gamma_{s,n,kum}(t) = g_{s,n,kum}(t)/N_0$ is the signal-to-noise ratio (SNR) of unit power between the n th USV and the s th MS. N_0 is the noise power. Similarly, for the n th USV, the achievable data rate between the s th MS and OBS is expressed as

$$R_{s,kmo}(t) = B \log_2 \left(1 + \sum_{k=1}^K \theta_{n,k}(t) q_{s,k}(t) \gamma_{s,kmo}(t) \right) \quad (3)$$

where $q_{s,k}$ is the transmit power on the k th channel for the s th MS. $\gamma_{s,kmo}(t) = g_{s,kmo}(t)/N_0$ is the SNR of unit power between the s th MS and OBS. Putting all mentions together, the achievable two-hop data rate of n th USV can be written as

$$R_n(t) = \sum_{s=1}^S \sum_{k=1}^K \delta_{s,n}(t) \cdot \min\{R_{s,n,kum}(t), R_{s,kmo}(t)\}. \quad (4)$$

B. AoI-Penalty-Aware State Estimation

At the remote end, OBS receives the sensory data and then estimates the system state such that the transmission performance of sensing data directly affects the estimation performance. In this regard, the concept of AoI is introduced to capture the delay experience for the application of state estimation due to the imperfect wireless transmission. Take the end-to-end transmission between the n th USV and the OBS for example. The binary variable $\chi_n(t)$ is introduced to indicate that whether the end-to-end transmission of the n th USV at the time step t is successful or not. If the data packet is delivered in the time step t , $\chi_n(t) = 1$. Otherwise, $\chi_n(t) = 0$. Correspondingly

$$\chi_n(t) = \begin{cases} 1, & \text{if } R_n(t)\Delta \geq l_n(t) \\ 0, & \text{otherwise} \end{cases} \quad (5)$$

where Δ is the duration of one time step. It can be seen that $\chi_n(t)$ depends on the achievable end-to-end data rate $R_n(t)$, which, in turn, is determined by the transmit power p and q , association relationship, channel allocation θ , and MSs' locations \mathbf{z}_s . If the transmission of data packet is accomplished

before the end of time step t , the AoI is the transmission delay $\lceil [l_n(t)/(R_n(t)\Delta)] \rceil$, where the value of $R_n(t)\Delta$ denotes the delivered data volume at time step t . Then, the AoI of data packet generated by the n th USV at time t is

$$\tau_n(t) = \begin{cases} \lceil \frac{l_n(t)}{R_n(t)\Delta} \rceil, & \text{if } \chi_n(t) = 1 \\ \tau_n(t-1) + 1, & \text{if } \chi_n(t) = 0. \end{cases} \quad (6)$$

The expectation of AoI is used to emulate the experienced delay (i.e., average AoI of sensory data), which is given by $\mathbb{E}\{\tau_n(t)\} = \Pr\{\chi_n(t) = 1\} \lceil [l_n(t)/(R_n(t)\Delta)] \rceil + \Pr\{\chi_n(t) = 0\}(\mathbb{E}\{\tau_n(t-1)\} + 1)$. The state estimation is convergent [35], if

$$\Pr\{\chi_n(t) = 0\} \leq \frac{1}{\rho(A)^2}. \quad (7)$$

Assuming that the latest received state information at the OBS is $\mathbf{x}_n(t - \tau_n(t))$, (1) could be written as

$$\mathbf{x}_n(t) = A^{\tau_n(t)} \mathbf{x}_n(t - \tau_n(t)) + \sum_{m=1}^{\tau_n(t)} A^{m-1} \mathbf{v}_n(t - m). \quad (8)$$

According to [31], the OBS estimates the system state with received sensory information, and the estimate is given by

$$\hat{\mathbf{x}}_n(t) = A^{\tau_n(t)} \mathbf{x}_n(t - \tau_n(t)) \quad (9)$$

where $\mathbf{x}_n(t - \tau_n(t))$ is the latest state information received by OBS. The estimation performance is evaluated by the estimation distortion, which is expressed as a function of AoI-based estimation error

$$\mathbf{e}_n(t) = \mathbf{x}_n(t) - \hat{\mathbf{x}}_n(t) = \sum_{m=1}^{\tau_n(t)} A^{m-1} \mathbf{v}_n(t - m). \quad (10)$$

From the perspective of state estimation, the MSE is employed to evaluate the estimation performance and given by

$$\mathbb{E}\{\|\mathbf{e}_n(t)\|_2^2\} = \mathbb{E}\left\{ \sum_{m=1}^{\tau_n(t)-1} \text{Tr} \left((A^T)^m A^m Q_n \right) \right\} = \mathcal{G}(\tau_n(t)) \quad (11)$$

where $\tau_n(t)$ is the only time-dependent variable. Note that $\mathcal{G}(\tau_n(t))$ is an increasing function with respect to $\tau_n(t)$ when the spectral radius of plant A is larger than one. This motivates us to investigate how to reduce the average AoI of sensory data with limited resources to enhance the estimation performance.

C. Problem Formulation

In order to improve the adaptability of monitoring missions to the system dynamics and resource limitation, the MS location, USV association, channel allocation, and transmit power are jointly designed to reduce the estimation distortion for all USVs. In the duration of T time steps, the interested problem about the communication resources and estimation convergence constrained problem is mathematically reformulated as

$$\mathcal{P}_1 : \min_{\{\mathbf{z}_s, \delta, \theta, p, q\}} \frac{1}{T} \sum_{t=1}^T \sum_{n=1}^N \ln \left[\Gamma^{\mathbb{E}\{\tau_n(t)\}} \cdot \mathcal{G}(\tau_n(t)) \right] \quad (12)$$

$$\text{s.t. } \sum_{s=1}^S \delta_{s,n}(t) = 1 \quad \forall n \in \mathcal{N} \quad (12a)$$

$$\sum_{n=1}^N \theta_{n,k}(t) \leq 1 \quad \forall k \in \mathcal{K} \quad (12b)$$

$$\sum_{k=1}^K \theta_{n,k}(t) q_{s,n,k}(t) \leq q_{\max} \quad \forall n \in \mathcal{N} \quad \forall s \in \mathcal{S} \quad (12c)$$

$$\sum_{k=1}^K \theta_{n,k}(t) p_n(t) \leq p_{\max} \quad \forall n \in \mathcal{N} \quad (12d)$$

$$\Pr\{R_n(t) \geq l_n(t)/\Delta\} \geq 1 - \frac{1}{\rho^2(A)} \quad \forall n \in \mathcal{N} \quad (12e)$$

where q_{\max} and p_{\max} are the maximum transmit power of MS and USV, respectively. The sum of logarithmic function $\ln(\cdot)$ in the objective function guarantees both the fairness and the overall performance; (12a) denotes one USV can be associated to no more than one MS; (12b) denotes that a channel can be allocated to at most one USV; (12c) and (12d) are the transmit power constraint of MS and USV, respectively; and (12e) is the estimation convergence condition that is heavily effected by the transmission performance. $\Gamma^{\mathbb{E}\{\tau_n(t)\}}$ is employed to adjust the penalty degree of experienced delay. As Γ approaches to one, the scheduler has the similar preferences for young and old AoI, which could be regarded as the finite-time average estimation distortion. On the contrary, when Γ is much larger than one, the scheduler weights more on the penalty of old AoI. It means that the considered network system has more stringent requirement on the old AoI of sensory data.

IV. JOINT OPTIMIZATION OF MS LOCATION, CHANNEL ALLOCATION, AND TRANSMIT POWER

It is of importance to note that the formulated problem (12) is a mixed-integer nonlinear programming (MINLP) problem, since it includes the binary association indicator δ , binary channel allocation variable θ , and continuous transmit power variables p and q . The nonlinear objective function cannot be expressed explicitly with decision variables. Thus, the effective decomposition and iterative methods are employed to solve (12) effectively. Therefore, we investigate the joint optimization of location and association by ignoring the heterogeneities of wireless channels and transmit power. Subsequently, the channel allocation and transmit power are designed to further reduce the end-to-end transmission latency for enhancing the state estimation performance.

Let $\mathcal{T}_n = \text{Tr}(A^T A Q_n)$, then (11) is equal to $\mathcal{G}(\tau_n(t)) = [((\mathcal{T}_n)^{\mathbb{E}\{\tau_n(t)\}} - 1)/(\mathcal{T}_n - 1)]$. The objective function is rewritten as $\ln((\Gamma)^{\mathbb{E}\{\tau_n(t)\}} \cdot [((\mathcal{T}_n)^{\mathbb{E}\{\tau_n(t)\}} - 1)/(\mathcal{T}_n - 1)]) = \mathbb{E}\{\tau_n(t)\} \ln(\Gamma) + \ln((\mathcal{T}_n)^{\mathbb{E}\{\tau_n(t)\}} - 1) - \ln(\mathcal{T}_n - 1)$, which approximates to $\mathbb{E}\{\tau_n(t)\} \ln(\Gamma \cdot \mathcal{T}_n) - \ln(\mathcal{T}_n - 1)$. In this regard, the objective function is approximated to $(1/T) \sum_{t=1}^T \sum_{n=1}^N \mathbb{E}\{\tau_n(t)\} \ln(\Gamma \cdot \mathcal{T}_n) - \ln(\mathcal{T}_n - 1)$, where time accumulated objective function makes it challenging to solve this mixed-integer nonlinear problem effectively. For

the convenience of tackling this problem, we focus on the subproblem at each time step with the objective function $\sum_{n=1}^N \mathbb{E}\{\tau_n(t)\} \ln(\Gamma \cdot \mathcal{T}_n) - \ln(\mathcal{T}_n - 1)$. Moreover, it can be seen that the objective function linearly increases with the growth of AoI. Hence, we will pay effort to reduce the AoI by jointly optimizing the MS location, USV association, channel allocation, and transmit power.

A. Joint Design of MSs' Location and USV Association

In particular, the joint optimization subproblem of MS location and USV association at the t th time step is given by

$$\begin{aligned} \mathcal{P}_2 : \min_{\{\mathbf{s}, \delta\}} & \sum_{n=1}^N \mathbb{E}\{\tau_n(t)\} \ln(\Gamma \cdot \mathcal{T}_n) - \ln(\mathcal{T}_n - 1) \\ \text{s.t. } & (12a), (12e) \end{aligned} \quad (13)$$

where $\mathbb{E}\{\tau_n(t)\} = \Pr\{R_n(t) \geq l_n(t)/\Delta\} + (1 - \Pr\{R_n(t) \geq l_n(t)/\Delta\})(\mathbb{E}\{\tau_n(t-1)\} + 1) = -\mathbb{E}\{\tau_n(t-1)\} \Pr\{R_n(t) \geq l_n(t)/\Delta\} + (\mathbb{E}\{\tau_n(t-1)\} + 1)$ and $\mathbb{E}\{\tau_n(t-1)\}$ is a constant known at the t th time step. Since $\mathbb{E}\{\tau_n(t-1)\} > 0$, it can be seen that this objective function decreases with the growth of the rate of packet success transmission (RPST). Moreover, the RPST is proportional to the end-to-end data rate $R_n(t)$, which could be expressed as $R_n(t) = \{\min\{R_{s,n,k_{um}}(t), R_{s,k_{mo}}(t)\} | \delta_{s,n}(t) = 1, \theta_{n,k}(t) = 1\}$.

1) *USV Association With Given MSs' Location*: Since the path loss depends on the propagation distance, the association between USVs and MSs is determined by the distance between them. Moreover, because USVs have different effects on the estimation performance, the MS will select USVs in terms of \mathcal{T}_n that is constrained by the MS-OBS transmission capacity. The transmission capacity depends on the assigned channels, which is elaborated in the next section. In order to determine the association between USVs and MSs at the t th time step, we design a heuristic algorithm based on the many-to-one matching theory [36], [37], shown as Algorithm 1. The main idea of Algorithm 1 is to obtain the better matching between USVs and MSs. In particular, we first obtain the preference lists for each MS and each USV, respectively. Then, the best ω_s USVs are added into the candidate set of associated USVs for the s th MS. Finally, we assess whether a USV is associated to multiple MSs. If the USV is added into more than one candidate set, it will be removed from the candidate sets of MSs that does not have the largest preference factor.

Theorem 1: The complexity of Algorithm 1 is polynomial.

Proof: We first obtain the preference lists for each MS and each USV according to steps 4–6 and steps 7–9, respectively. The time complexity of steps 4–6 and steps 7–9 is $\mathcal{O}(SN \log(N))$ and $\mathcal{O}(NS \log(S))$, respectively. Then, we add the best ω_s USVs into the candidate set of s th MS, and the time complexity of steps 10–17 is $\mathcal{O}(S)$. If the USV is added into more than one candidate set, it will be removed from the candidate sets of MSs that does not have the largest preference factor. The time complexity of steps 18–28 is $\mathcal{O}(NS)$. In summary, the time complexity is $\mathcal{O}(SN \log(N))$, and the designed heuristic algorithm is a polynomial time algorithm. ■

2) *MSs' Location Optimization for the Associated USV*: In this problem, the locations of MSs determine the channel gain,

Algorithm 1 Each MS Selects the Associated USVs

```

1: Input: the MS-OBS transmission capacity  $\mathbb{R}_s$  for
   each MS, the number of associated USVs  $\omega_s = \sum_{n \in \mathcal{N}} \sum_{k \in \mathcal{K}} \mathbb{I}(\theta_{n,k} q_{s,n,k}(t))$ , and the location of OBS,
   MS, USV are  $\mathbf{z}_0$ ,  $\mathbf{z}_s$ ,  $\mathbf{z}_n$ , respectively;
2: Output: the USV association relationship  $\delta$ ;
3: Initialize the association indication  $\delta = \emptyset$ ;
4: for Each MS  $s \in \mathcal{S}$  do
5:   Sort all USVs in the nondecreasing order with respect to
      $T_n$ , and the indicator of the  $M$ -th element in the ordered
     nondecreasing sequence  $l_s$  is  $I_s(M)$ ;
6: end for
7: for Each USV  $n \in \mathcal{N}$  do
8:   Sort all MSs in the nondecreasing order with respect to
     the distance  $\|\mathbf{z}_s - \mathbf{z}_n\|_2^2$ , and the ordered nondecreasing
     sequence  $l_n$ ;
9: end for
10: for Each MS  $s \in \mathcal{S}$  do
11:    $F_s \leftarrow 0$ ,  $L_s \leftarrow \emptyset$ ,  $J_s \leftarrow \emptyset$  and  $M_s \leftarrow |J_s|$ ;
12:   while  $M_s < \omega_s - |J_s|$  do
13:      $M_s \leftarrow M_s + 1$ ;
14:      $L_s \leftarrow L_s \cup l_s(M_s)$ ;
15:      $\delta_{s,l_s(M_s)} \leftarrow 1$ ;
16:   end while
17: end for
18: for Each USV  $n \in \mathcal{N}$  do
19:   if  $\sum_{s \in \mathcal{S}} \sum_{l_s(M_s)=1} \delta_{s,l_s(M_s)} > 1$  then
20:      $[s_n, n_s] \leftarrow \arg \min_{s \in \mathcal{S}} \{\|\mathbf{z}_s - \mathbf{z}_n\|_2^2\}$ ;
21:      $\delta_{s_n, n_s} \leftarrow 1$ ;
22:     for Each MS  $s \in \mathcal{S}$  do
23:       if  $l_s(M_s) \neq n_s$  then
24:          $L_s \leftarrow L_s \setminus l_s(M_s)$  and  $\delta_{s,l_s(M_s)} \leftarrow 0$ ;
25:       end if
26:     end for
27:   end if
28: end for
29: for Each MS  $s \in \mathcal{S}$  do
30:    $L_s \leftarrow J_s$ ;
31: end for
32: if  $\prod_{n \in \mathcal{N}} (\sum_{s \in \mathcal{S}} \delta_{s,n}) \neq 1$  then
33:   Go to step 4;
34: else
35:   Return  $\delta$ ;
36: end if

```

which further effects the USV-MS transmission capacity and the MS-OBS transmission capacity. The MS location is optimized by maximizing the sum rate of all associated USV with given channel allocation and power control. The MS location optimization problem is given by

$$\mathcal{P}_3 : \min_{\{\mathbf{z}_s\}} \sum_{n=1}^N \mathbb{E}\{\tau_n(t)\} \ln(\Gamma \cdot T_n) - \ln(T_n - 1) \quad \text{s.t. (12e)} \quad (14)$$

where the complicated relationship between $\mathbb{E}\{\tau_n(t)\}$ and the MS location \mathbf{z}_s makes it difficult to solve this problem directly. As a solution, the upper bound of the objective function is studied to obtain the worse case solution of this problem. This worse case problem is formulated as

$$\min_{\{\mathbf{z}_s\}} \sum_{n=1}^N 1/R_n(t) \cdot \left(1 - 1/\rho^2(A)\right) (l_n(t)/\Delta) \ln(\Gamma \cdot T_n) + \left(1/\rho^2(A)\right) (\mathbb{E}\{\tau_n(t-1)\} + 1) \ln(\Gamma \cdot T_n) - \ln(T_n - 1). \quad (15)$$

According to (2)–(4), it yields that $R_{s,n,k_{um}}(t) = B \log_2(1 + [(p_n(t)h_{s,n,k_{um}}G_{s,n_{tx}}G_{s,n_{rx}}\varsigma d_0^2)/(16\pi^2 N_0)]) \cdot [1/(\|\mathbf{z}_s(t) - \mathbf{z}_n(t)\|_2^2)]$, which is approximated to $R_{s,n,k_{um}}(t) = [(B\kappa_{s,n,k_{um}}(t))/(\|\mathbf{z}_s(t) - \mathbf{z}_n(t)\|_2^2)]$ with $\kappa_{s,n,k_{um}}(t) = [(p_n(t)h_{s,n,k_{um}}G_{s,n_{tx}}G_{s,n_{rx}}\varsigma d_0^2)/(16\pi^2 N_0)]$. Similarly, $R_{s,n,k_{mo}}(t)$ is approximated to $[(B\kappa_{s,n,k_{mo}}(t))/(\|\mathbf{z}_s(t) - \mathbf{z}_0(t)\|_2^2)]$ with $\kappa_{s,n,k_{mo}}(t) = [(q_{s,n,k}(t)h_{s,n,k_{mo}}G_{s,0_{tx}}G_{s,0_{rx}}\varsigma d_0^2)/(16\pi^2 N_0)]$.

For the case that $R_{s,n,k_{um}}(t) \leq R_{s,n,k_{mo}}(t)$, $R_n(t) = R_{s,n,k_{um}}(t)$ and $1/R_n(t) = [(\|\mathbf{z}_s(t) - \mathbf{z}_n(t)\|_2^2)/(B\kappa_{s,n,k_{um}}(t))]$. Then, (15) is reformulated as

$$\mathcal{P}_4 : \min_{\{\mathbf{z}_s\}} \sum_{n=1}^N \frac{\|\mathbf{z}_s(t) - \mathbf{z}_n(t)\|_2^2}{B\kappa_{s,n,k_{um}}(t)} \cdot \zeta_1 + \zeta_2 \quad (16)$$

where $\zeta_1 = (1 - 1/\rho^2(A))(l_n(t)/\Delta) \ln(\Gamma \cdot T_n)$ and $\zeta_2 = (1/\rho^2(A))(\mathbb{E}\{\tau_n(t-1)\} + 1) \ln(\Gamma \cdot T_n) - \ln(T_n - 1)$.

If $R_{s,n,k_{um}}(t) > R_{s,n,k_{mo}}(t)$, then we can obtain $R_n(t) = R_{s,n,k_{mo}}(t)$ and $1/R_n(t) = [(\|\mathbf{z}_s(t) - \mathbf{z}_0(t)\|_2^2)/(B\kappa_{s,n,k_{mo}}(t))]$. In this case, (15) is transformed to

$$\mathcal{P}_5 : \min_{\{\mathbf{z}_s\}} \sum_{n=1}^N \frac{\|\mathbf{z}_s(t) - \mathbf{z}_n(t)\|_2^2}{B\kappa_{s,n,k_{mo}}(t)} \cdot \zeta_1 + \zeta_2. \quad (17)$$

As the objective functions of (16) and (17) are in 2-norm, \mathcal{P}_4 and \mathcal{P}_5 are unconstrained convex programming. Therefore, the KKT conditions are used to obtain the optimal solutions of \mathcal{P}_4 and \mathcal{P}_5 .

As the MS location adjustment may change the clustering result, it is necessary to execute the USV association and the MS location optimization in an iterative manner.

B. AoI-Aware Channel Allocation With Power Control

In this section, we design the channel allocation among USV-MS links in each group to achieve the reliable and low-latency data transmission for multiple sensing missions simultaneously.

1) *Channel Allocation With Power Control Among the Associated USVs for Each MS:* The optimization problem is

$$\mathcal{P}_6 : \min_{\{\theta, q\}} \sum_{n=1}^N \mathbb{E}\{\tau_n(t)\} \ln(\Gamma \cdot T_n) - \ln(T_n - 1) \quad \text{s.t. (12b), (12c).} \quad (18)$$

Algorithm 2 is designed to solve the problem (18) with given transmit power q . The main idea of Algorithm 2 is to allocate each channel to the best MS and USV in terms of

Algorithm 2 Channel Allocation Among Associated USVs

- 1: **Input:** The USV association $\delta_{n,s}$, the number of associated USVs for each MS $\nu_s = \sum_n \delta_{n,s}$, and the SNR of the k th channel for USV-MS link and MS-OBS link $\gamma_{n,s,k_{um}}(t)$ and $\gamma_{s,k_{mo}}(t)$;
- 2: **Output:** the channel allocation θ ;
- 3: Initialize the channel allocation indication $\theta = \emptyset$, and $\varsigma_s = 0$;
- 4: Each MS $s \in \mathcal{S}$ sorts all channels in the nonincreasing order with respect to $R_{s,k_{mo}}(t)$ (shown as (3)), the ordered nonincreasing sequence is denoted as \mathcal{K}_s ;
- 5: **for** Each channel $k \in \mathcal{K}$ **do**
- 6: **for** Each MS $s \in \mathcal{S}$ **do**
- 7: **if** $k == \mathcal{K}_s(1)$ and $\varsigma_s < \nu_s$ **then**
- 8: $\vartheta_{s,k} = 1$;
- 9: **if** $\sum_s \vartheta_{s,k} > 1$ **then**
- 10: $s_k = \arg \max_{s \in \mathcal{S}} R_{s,k_{mo}}(t)$
- 11: $\vartheta_{s,k} = 1$ for $s == s_k$, and $\vartheta_{s,k} = 0$ for $s \neq s_k$;
- 12: $\mathcal{K}_s = \mathcal{K}_s \setminus \mathcal{K}_s(1)$;
- 13: $\varsigma_s = \varsigma_s + 1$;
- 14: **end if**
- 15: **end if**
- 16: **end for**
- 17: **end for**
- 18: **for** Each MS $s \in \mathcal{S}$ **do**
- 19: **for** The channel $\{k | \vartheta_{s,k} == 1, k \in \mathcal{K}\}$ **do**
- 20: $k_n = \arg \max_{\{n | \delta_{n,s}=1\}} R_{n,s,k_{um}}(t)$;
- 21: **for** Each USV $n \in \mathcal{N}$ **do**
- 22: **if** $n == k_n$ **then**
- 23: $\theta_{n,k} = 1$;
- 24: **else**
- 25: $\theta_{n,k} = 0$;
- 26: **end if**
- 27: **end for**
- 28: **end for**
- 29: **end for**
- 30: Return θ ;

the available data rate. In particular, to choose the best MS for each channel, each MS choose the first element of the ordered nonincreasing sequence \mathcal{K}_s . If more than one MSs choose the k th channel, we will choose the best MS (s_k) in terms of the available data rate ($R_{s,k_{mo}}(t)$), and remove the k th channel from the ordered channel list \mathcal{K}_s . Moreover, in order to choose the best USV for the k th channel, we search all USVs that are associated to the MS (s_k), and find out the best USV (k_n) in terms of the available data rate ($R_{n,s,k_{um}}(t)$). The detailed algorithm is shown as below. In Algorithm 2, the computational complexity of sorting all channels in the nonincreasing order in step 4 is $\mathcal{O}(S \log(S))$. As the complexity of finding out the UVS with the largest throughput in step 10 is $\mathcal{O}(S)$, the complexity of steps 5–17 is $\mathcal{O}(S^2K)$. Similarly, the complexity of steps 18–29 is $\mathcal{O}(SNK)$. In summary, the complexity of Algorithm 2 is $\mathcal{O}(SNK)$. In order to further decrease the value of the objective function, the transmit power is optimized on the assigned channel with the water-filling

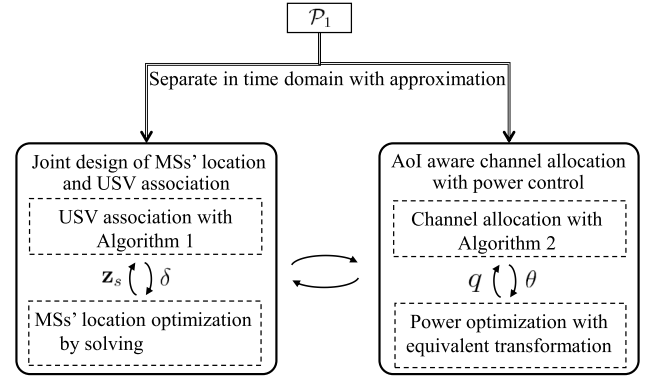


Fig. 3. Diagram of solution process.

algorithm. The channel allocation algorithm and the power control algorithm are executed iteratively until the gap between adjacent iterations is small enough.

2) *Transmit Power Optimization for USVs:* As $R_n(t) = \{\min\{R_{s,n,k_{um}}(t), R_{s,k_{mo}}(t) | \delta_{s,n}(t) = 1, \theta_{n,k}(t) = 1\}$, the maximum value of $R_n(t)$ will be reached, if $\{R_{s,n,k_{um}}(t) = R_{s,k_{mo}}(t) | \delta_{s,n}(t) = 1, \theta_{n,k}(t) = 1\}$. According to (2) and (3), this condition is mathematically equivalent to $p_{n,k}(t)\gamma_{s,n,k_{um}}(t) = q_{s,n,k}(t)\gamma_{s,k_{mo}}(t)$. It yields that

$$\frac{d_{s,0}^2(t)}{d_{s,n}^2(t)} = \frac{q_{s,n,k}(t)}{p_{n,k}(t)} \frac{G_{s,0_{tx}}G_{s,0_{rx}}h_{s,k_{mo}}}{G_{s,n_{tx}}G_{s,n_{rx}}h_{s,n,k_{um}}}. \quad (19)$$

Equation (19) indicates that the adjustment of MSs' locations depends on the relative transmit power of MS and its associated USV. The maximum value of $q_{s,n,k}(t)$ and $p_{n,k}(t)$ is q_{\max} and p_{\max} , respectively. Then, we can obtain the transmit power of the associated USV with given $q_{s,n,k}(t)$, which is expressed as

$$p_{n,k}(t) = q_{s,n,k}(t) \frac{d_{s,n}^2(t)}{d_{s,0}^2(t)} \frac{G_{s,0_{tx}}G_{s,0_{rx}}h_{s,k_{mo}}}{G_{s,n_{tx}}G_{s,n_{rx}}h_{s,n,k_{um}}}. \quad (20)$$

If $\sum_{k=1}^K \theta_{n,k}(t)p_{n,k}(t) > p_{\max}$, the value of $q_{s,n,k}(t)$ is reset to be $q_{s,n,k}(t) = [(d_{s,0}^2(t))/(d_{s,n}^2(t))] [(G_{s,n_{tx}}G_{s,n_{rx}}h_{s,n,k_{um}})/(G_{s,0_{tx}}G_{s,0_{rx}}h_{s,k_{mo}})] [p_{\max}/(\sum_{k=1}^K \theta_{n,k}(t)p_{n,k}(t))]$.

The initial values of USV's transmit power are set to be $p_{n,k}(t) = (p_{\max}/K) \forall n \in \mathcal{N}$, and the initial values of MS's transmit power are set to be $q_{s,n,k}(t) = (q_{\max}/K) \forall n \in \mathcal{N} \forall s \in \mathcal{S}$, where K is the number of channels. The initial values of channel allocation are set based on the random scheme. In particular, the USVs in set \mathcal{N} randomly choose an available channel in sequence. If the channel is chosen by an USV, this channel is considered to be unavailable for subsequent USVs. The original problem is solved by solving two problems iteratively. One problem is to optimize channel allocation and power control, and the other is to jointly design the MS locations and UAV association.

The diagram of solution process is shown as Fig. 3. The complexity of USV's power control is $\mathcal{O}(S^{3.5})$, when the interior point method is applied for convex programming [38]. After the initialization, Algorithm 1 and power control algorithm alternately perform the USV association algorithm and location adjustment algorithm, until the convergence condition

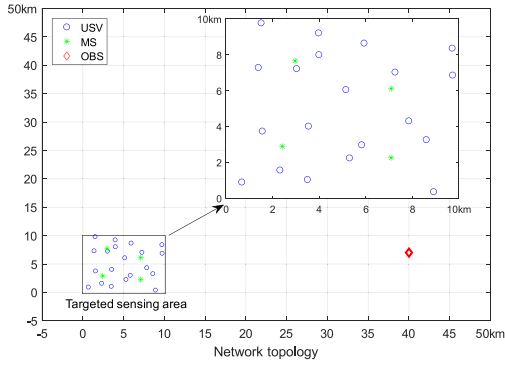


Fig. 4. Network topology.

TABLE I
MAIN PARAMETERS

Parameters	Values
Reference distance d_0	1 m
Path loss at the reference distance PL_0	56.7 dB
Noise power N_0	-87 dBm
Path loss exponent n	2.31
Small-scale fading distribution between USV and MS	Rayleigh (0,1)
Small-scale fading distribution between MS and OBS	Rice (0,1)
Maximum transmit power of USV	10 mw
Maximum transmit power of MS	50 mw
Bandwidth of each channel B	0.2 MHz
Sampling interval of the estimator Δ	100 ms

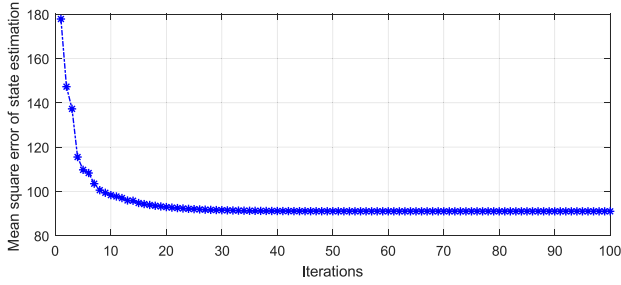


Fig. 5. Diagram of convergence.

is met or the maximum number of iteration M_1 is achieved. The computational complexity of this iteration process is $\mathcal{O}(S^{4.5}N \log(N)M_1)$. Similarly, Algorithm 2 and power control algorithm alternately perform the channel algorithm and power control algorithm, until the convergence condition is met or the maximum number of iteration M_2 is achieved. The computational complexity of this iteration process is $\mathcal{O}(S^2NKM_2)$. After optimizing channel allocation and power control, the MS locations and UAV association should be adjusted. The original problem is solved by solving two problems iteratively, until the convergence condition is met or the maximum number of iteration M_0 is achieved. Therefore, the computational complexity of the overall scheme is $\mathcal{O}(S^{4.5}N \log(N)M_1M_0 + S^2NKM_2M_0)$.

V. PERFORMANCE EVALUATION

In this section, we conduct extensive simulations to evaluate the performance of the proposed location-dependent cooperative transmission (LDCT) for AoI-plenty-aware state estimation in marine IoT systems. Two other schemes are

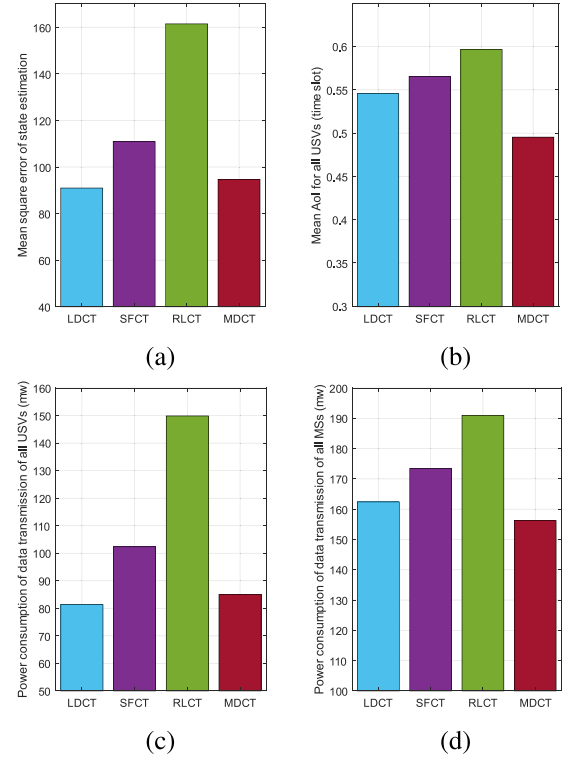


Fig. 6. Energy consumption comparison among different schemes. (a) Estimation error. (b) Mean AoI. (c) USVs' energy consumption. (d) MSs' energy consumption.

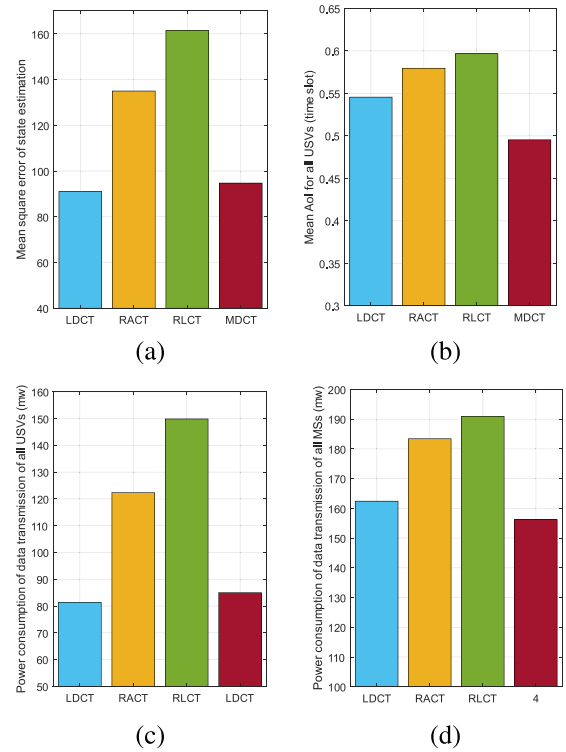


Fig. 7. Energy consumption comparison among different schemes. (a) Estimation error. (b) Mean AoI. (c) USVs' energy consumption. (d) MSs' energy consumption.

implemented in the following simulations for comparison purpose. One is called the randomly located cooperative transmission (RLCT) scheme for AoI-plenty-aware state

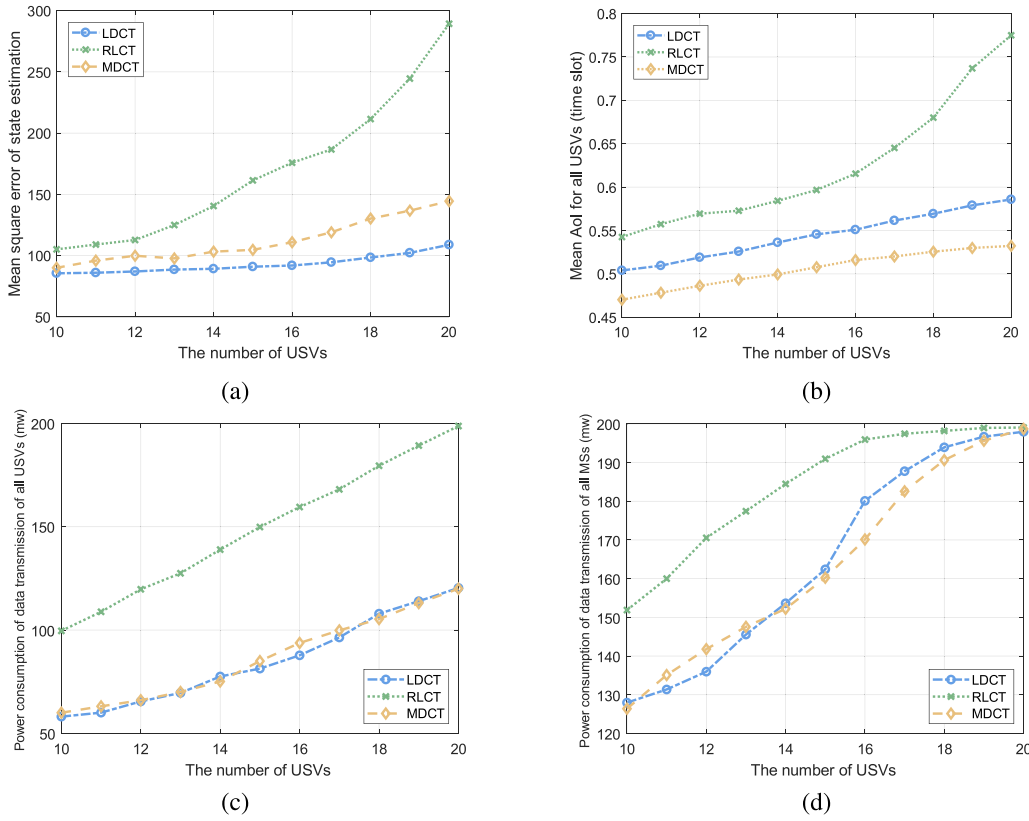


Fig. 8. Performance comparison with different numbers of USVs. (a) Estimation error. (b) Mean AoI. (c) Energy consumption of USVs' data transmission. (d) Energy consumption of MSs' data transmission.

estimation, wherein MSs are randomly located in the monitoring area and the location adjustment of MSs is not considered. The other is called the minimized experienced delay cooperative transmission (MDCT) scheme, which aims to minimize the sum age of sensory data collected by all USVs. For more convincing, we consider another compared scheme, called the strong signal first cooperative transmission (SFCT) scheme [39], [40]. With the SFCT scheme, MS adjusts the location based on the average strength of the signals received from all associated USVs. Moreover, the random channel allocation-based cooperative transmission (RACT) scheme is also considered for AoI-plenty-aware state estimation, wherein the subchannels are randomly allocated to USVs without considering the channel allocation optimization.

The case study considered in this article is the seawater temperature monitoring, which is a typical case of the marine environment in smart ocean. The scheme performance is evaluated according to the network topology covering a rectangular area $[0, 10]_{\text{km}} \times [0, 10]_{\text{km}}$, wherein $N = 20$ USV and $S = 4$ MS are placed, shown as Fig. 4. In simulation, the number of channels is set to be 20, and other main parameters used are shown in Table I. Set the initial state covariance matrix and the initial error covariance matrix as $W_0 = 10\mathbf{I}$ and $Q = 10\mathbf{I}$, respectively, where \mathbf{I} is a unit diagonal matrix [21].

A. Performance Evaluation Among Three Compared Schemes

Although the channel allocation and power control problem is a mixed-integer optimization problem, Fig. 5 validates that

the iteration is converged. The proposed LDCT scheme is almost convergent when the number of iterations is 30. The convergence rate is acceptable.

The MSE of state estimation and the mean AoI for all monitoring applications is shown as Fig. 6(a) and (b), respectively. We can find that the MSE and AoI with the RLCT scheme are much larger than that with the other three schemes. It verifies the superiority and shows the significance of joint design of cooperative transmission and location adjustment for the considered marine IoT system. Furthermore, it can be seen that the mean AoI with the MDCT scheme is lowest, but the MSE of state estimation with it is larger than that with the LDCT scheme. It reveals that although the AoI of received sensing data has impact on the estimation performance, it is not quite suitable to directly employ the AoI to evaluate the estimation performance for monitoring applications. Instead, the integration of classic MSE and mean AoI could appropriately characterize the impact of transmission delay and packet loss on the estimation performance.

Considering the limitation of energy resource, the transmit power consumption caused by the data transmission of all USVs and MSs is shown as Fig. 6. It reveals that the power consumption of data transmission with the SFCT scheme is better than that with the RLCT scheme, but worse than that with the LDCT scheme. Moreover, the transmit power consumed by the data transmission of all USVs and MSs with the RLCT scheme is much larger, mainly because that the MS location is not optimized together with the data transmission.

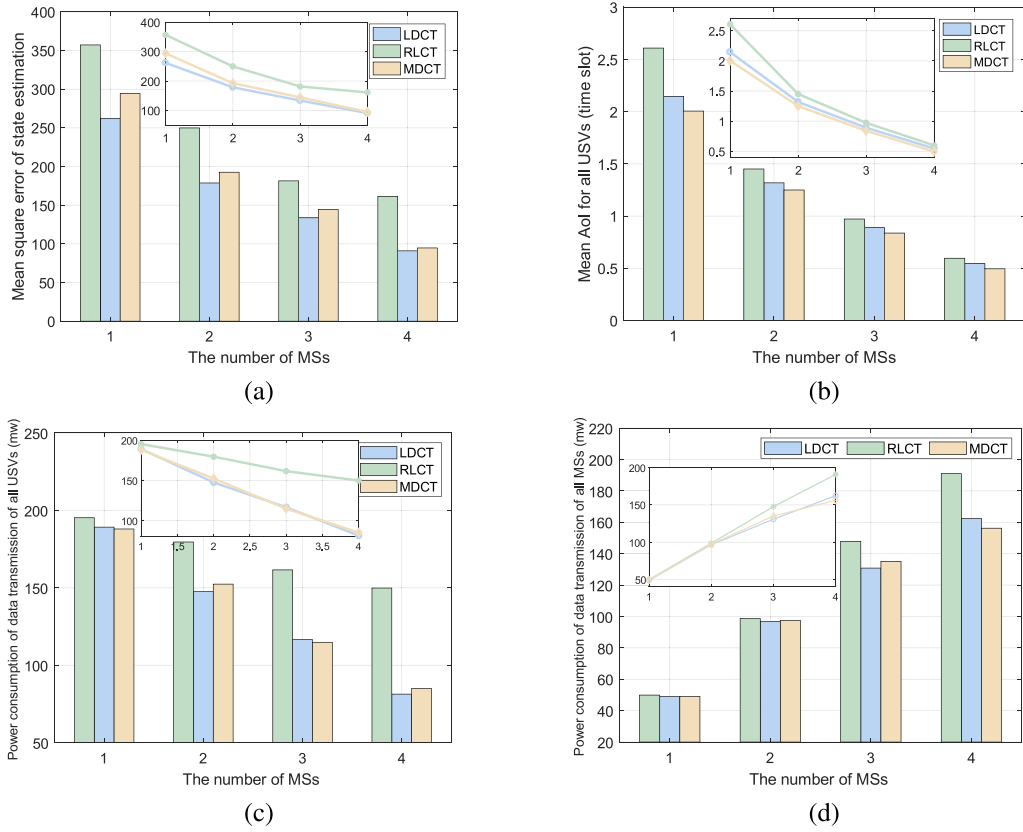


Fig. 9. Energy consumption comparison with different numbers of MSs. (a) Estimation error. (b) Mean AoI. (c) Energy consumption of USVs' data transmission. (d) Energy consumption of MSs' data transmission.

In a worse case that all MSs are far from the USVs and OBS, due to the location adjustment is out of consideration, the RLCT scheme has to increase the transmit power to compensate the effect of path loss and fading on the strength of received signal to meet the transmission requirements of monitoring applications.

Fig. 7 shows that the proposed channel allocation scheme is better than the random channel allocation scheme, in terms of the state estimation error, mean AoI, and the power consumption of data transmission.

B. Performance Comparison With Different Numbers of USVs and MSs

In Fig. 8, we evaluate the impact of the number of USVs on the scheme performance in terms of MSE, mean AoI, and power consumption. As shown in Fig. 8(a) and (b), the MSE of state estimation and AoI with LDCT and MDCT schemes increases slowly with the growth of the number of USVs. This is because that the larger the number of USVs is, the more transmit power will be consumed. Although the mean AoI with the MDCT scheme is lowest, the MSE of state estimation with LDCT is always smaller than that with MDCT. As shown in Fig. 8(c) and (d), both the LDCT and MDCT schemes could reduce the increase rate of transmit power consumption by optimizing the MS locations.

As shown in Fig. 9, we evaluate the impact of the number of MSs on the scheme performance in terms of MSE,

mean AoI, and power consumption. As shown in Fig. 9(a) and (b), the MSE of state estimation and mean AoI with LDCT and MDCT schemes is always much lower than that with the RLCT scheme. Moreover, the transmit power consumption with the MDCT scheme is much larger than that with the LDCT and RLCT schemes as the location adjustment is out of consideration, as shown in Fig. 9(c) and (d).

C. Estimation Performance Comparison With Different Maximum Transmit Power of USVs

The effect of maximum transmit power on the estimation is shown as Fig. 10. We can find that no matter what the number of MSs is, the estimation error with the LDCT scheme is always the smallest one, when the estimation error with the RLCT scheme is the largest one. Furthermore, the decreasing rate with the RLCT scheme is lower than that with both the LDCT and MDCT schemes. This performance improvement benefits from the joint design of cooperative transmission and location adjustment, making it possible to enhance the transmission performance for state estimation with limited resources. In particular, Fig. 10(b) and (c) clearly shows that the estimator error decreases with the growth of transmit power at the start, and then tends to be stable. The major reason is that the limited transmission capacity between MS and the OBS restricts the decreasing the AoI of information suffers over the MS-OBS link. Take the case of three MSs for example, the growth of the USV's transmit power make it possible

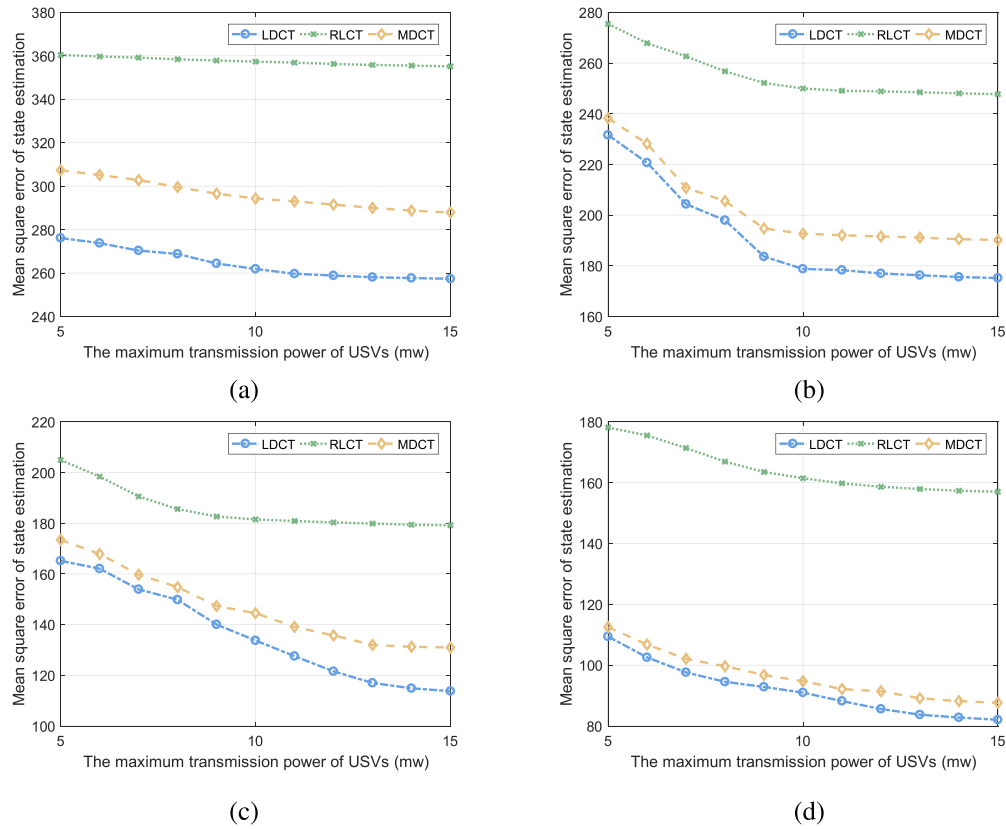


Fig. 10. Estimation error comparison with different maximum power. (a) Number of MSs = 1. (b) Number of MSs = 2. (c) Number of MSs = 3. (d) Number of MSs = 4.

to adjust the location of MSs to reduce the distance between MS and OBS. This action will increase the MS-OBS transmission capacity, and then decrease the estimation error. However, the superiority of increasing USV's transmit power will gradually disappear, especially, when the maximum transmit power is large. It means that only increasing the maximum transmit power of USVs cannot always reduce the estimation error under the constraint of transmit power.

VI. CONCLUSION

In this article, we have investigated the cooperative transmission for state estimation to achieve a high-reliable and low-latency data transmission for the environment monitoring in marine IoT systems. In particular, we have proposed a two-hop network architecture for marine IoT systems, where the MSs play the role of relay in the cooperative transmission. Under this architecture, the average AoI of sensory data is employed to characterize the impact of packets loss and transmission delay on the state estimation. Moreover, we have explored the relationship between MSE of state estimation and average AoI of sensory data. The AoI-plenty-aware state estimation and the MS-assisted cooperative transmission have been jointly designed and optimized to effectively reduce the effect of limited resources and path loss on the state estimation. Simulation results have demonstrated that the proposed LDCT scheme realizes smaller estimation error and lower power consumption, which is suited for the environment monitoring applications in marine IoT systems. For the future work,

we will investigate the problem of remote control for marine IoT systems over lossy wireless channels.

REFERENCES

- [1] X. Li, W. Feng, Y. Chen, C. Wang, and N. Ge, "Maritime coverage enhancement using UAVs coordinated with hybrid satellite-terrestrial networks," *IEEE Trans. Commun.*, vol. 68, no. 4, pp. 2355–2369, Apr. 2020.
- [2] J. H. Lee, J. Choi, W. H. Lee, J. W. Choi, and S. C. Kim, "Measurement and analysis on land-to-ship offshore wireless channel in 2.4 GHz," *IEEE Wireless Commun. Lett.*, vol. 6, no. 2, pp. 222–225, Apr. 2017.
- [3] D. Palma, "Enabling the maritime Internet of Things: CoAP and 6LoWPAN performance over VHF links," *IEEE Internet Things J.*, vol. 5, no. 6, pp. 5205–5212, Dec. 2018.
- [4] Y. Li, Y. Zhang, W. Li, and T. Jiang, "Marine wireless big data: Efficient transmission, related applications, and challenges," *IEEE Wireless Commun.*, vol. 25, no. 1, pp. 19–25, Feb. 2018.
- [5] J. Qiu, Z. Tian, C. Du, Q. Zuo, S. Su, and B. Fang, "A survey on access control in the age of Internet of Things," *IEEE Internet Things J.*, vol. 7, no. 6, pp. 4682–4696, Jun. 2020.
- [6] N. Cheng *et al.*, "Space/aerial-assisted computing offloading for IoT applications: A learning-based approach," *IEEE J. Sel. Areas Commun.*, vol. 37, no. 5, pp. 1117–1129, May 2019.
- [7] T. Wei, W. Feng, J. Wang, N. Ge, and J. Lu, "Exploiting the shipping lane information for energy-efficient maritime communications," *IEEE Trans. Veh. Technol.*, vol. 68, no. 7, pp. 7204–7208, Jul. 2019.
- [8] L. Lyu, C. Chen, S. Zhu, and X. Guan, "5G enabled codesign of energy-efficient transmission and estimation for industrial IoT systems," *IEEE Trans. Ind. Informat.*, vol. 14, no. 6, pp. 2690–2704, Jun. 2018.
- [9] Y. Xu, "Quality of service provisions for maritime communications based on cellular networks," *IEEE Access*, vol. 5, pp. 23881–23890, 2017.
- [10] N. Cheng *et al.*, "A comprehensive simulation platform for space-air-ground integrated network," *IEEE Wireless Commun.*, vol. 27, no. 1, pp. 178–185, Feb. 2020.

- [11] X. Shen and L. Deng, "A dynamic system approach to speech enhancement using the H/sub /spl infin// filtering algorithm," *IEEE Trans. Speech Audio Process.*, vol. 7, no. 4, pp. 391–399, Jul. 1999.
- [12] L. Lyu *et al.*, "Dynamics-aware and beamforming-assisted transmission for wireless control scheduling," *IEEE Trans. Wireless Commun.*, vol. 17, no. 11, pp. 7677–7690, Nov. 2018.
- [13] T. Sui, K. You, and M. Fu, "Stability conditions for multi-sensor state estimation over a lossy network," *Automatica*, vol. 53, pp. 1–9, Mar. 2015.
- [14] M. Rana, L. Li, and S. W. Su, "Distributed state estimation over unreliable communication networks with an application to smart grids," *IEEE Trans. Green Commun. Netw.*, vol. 1, no. 1, pp. 89–96, Mar. 2017.
- [15] Z. Xing and Y. Xia, "Distributed federated Kalman filter fusion over multi-sensor unreliable networked systems," *IEEE Trans. Circuits Syst. I, Reg. Papers*, vol. 63, no. 10, pp. 1714–1725, Oct. 2016.
- [16] X. Ren, J. Wu, K. H. Johansson, G. Shi, and L. Shi, "Infinite horizon optimal transmission power control for remote state estimation over fading channels," *IEEE Trans. Autom. Control*, vol. 63, no. 1, pp. 85–100, Jan. 2018.
- [17] H. Chen, C. Zhai, Y. Li, and B. Vucetic, "Cooperative strategies for wireless-powered communications: An overview," *IEEE Wireless Commun.*, vol. 25, no. 4, pp. 112–119, Aug. 2018.
- [18] N. T. Tuan, D.-S. Kim, and J.-M. Lee, "On the performance of cooperative transmission schemes in industrial wireless sensor networks," *IEEE Trans. Ind. Informat.*, vol. 14, no. 9, pp. 4007–4018, Sep. 2018.
- [19] T. Hiraguri *et al.*, "A cooperative transmission scheme in drone-based networks," *IEEE Trans. Veh. Technol.*, vol. 69, no. 3, pp. 2905–2914, Mar. 2020.
- [20] Z. Shi, S. Ma, H. ElSawy, G. Yang, and M.-S. Alouini, "Cooperative HARQ-assisted NOMA scheme in large-scale D2D networks," *IEEE Trans. Commun.*, vol. 66, no. 9, pp. 4286–4302, Sep. 2018.
- [21] L. Lyu, C. Chen, S. Zhu, N. Cheng, B. Yang, and X. Guan, "Control performance aware cooperative transmission in multiloop wireless control systems for industrial IoT applications," *IEEE Internet Things J.*, vol. 5, no. 5, pp. 3954–3966, Oct. 2018.
- [22] M. A. Abd-Elmagid, N. Pappas, and H. S. Dhillon, "On the role of age of information in the Internet of Things," *IEEE Commun. Mag.*, vol. 57, no. 12, pp. 72–77, Dec. 2019.
- [23] S. Kaul, R. Yates, and M. Gruteser, "Real-time status: How often should one update?" in *Proc. IEEE INFOCOM*, Orlando, FL, USA, Mar. 2012, pp. 2731–2735.
- [24] B. Zhou and W. Saad, "Joint status sampling and updating for minimizing age of information in the Internet of Things," *IEEE Trans. Commun.*, vol. 67, no. 11, pp. 7468–7482, Nov. 2019.
- [25] E. T. Ceran, D. Gündüz, and A. Gyöngy, "Average age of information with hybrid ARQ under a resource constraint," *IEEE Trans. Wireless Commun.*, vol. 18, no. 3, pp. 1900–1913, Mar. 2019.
- [26] Z. Wang, X. Qin, B. Liu, and P. Zhang, "Joint data sampling and link scheduling for age minimization in multihop cyber-physical systems," *IEEE Wireless Commun. Lett.*, vol. 8, no. 3, pp. 765–768, Jun. 2019.
- [27] I. Kadota, A. Sinha, and E. Modiano, "Scheduling algorithms for optimizing age of information in wireless networks with throughput constraints," *IEEE/ACM Trans. Netw.*, vol. 27, no. 4, pp. 1359–1372, Aug. 2019.
- [28] J. Wang, C. Jiang, K. Zhang, X. Hou, Y. Ren, and Y. Qian, "Distributed Q-learning aided heterogeneous network association for energy-efficient IIoT," *IEEE Trans. Ind. Informat.*, vol. 16, no. 4, pp. 2756–2764, Apr. 2020.
- [29] Z. Zhou *et al.*, "Energy-efficient resource allocation for energy harvesting-based cognitive machine-to-machine communications," *IEEE Trans. Cogn. Commun. Netw.*, vol. 5, no. 3, pp. 595–607, Sep. 2019.
- [30] M. K. Abdel-Aziz, S. Samarakoon, C.-F. Liu, M. Bennis, and W. Saad, "Optimized age of information tail for ultra-reliable low-latency communications in vehicular networks," *IEEE Trans. Commun.*, vol. 68, no. 3, pp. 1911–1924, Mar. 2020.
- [31] M. Klügel, M. H. Mamduhi, S. Hirche, and W. Kellerer, "AoI-penalty minimization for networked control systems with packet loss," in *Proc. IEEE Conf. Comput. Commun. Workshops (INFOCOM WKSHPS)*, Paris, France, 2019, pp. 189–196.
- [32] X. Xi, X. Cao, P. Yang, J. Chen, T. Quek, and D. Wu, "Joint user association and UAV location optimization for UAV-aided communications," *IEEE Wireless Commun. Lett.*, vol. 8, no. 6, pp. 1688–1691, Dec. 2019, doi: [10.1109/LWC.2019.2937077](https://doi.org/10.1109/LWC.2019.2937077).
- [33] R. Duan, J. Wang, H. Zhang, Y. Ren, and L. Hanzo, "Joint multicast beamforming and relay design for maritime communication systems," *IEEE Trans. Green Commun. Netw.*, vol. 4, no. 1, pp. 139–151, Mar. 2020.
- [34] J. Wang *et al.*, "Wireless channel models for maritime communications," *IEEE Access*, vol. 6, pp. 68070–68088, 2018.
- [35] B. Sinopoli, L. Schenato, M. Franceschetti, K. Poolla, M. I. Jordan, and S. S. Sastry, "Kalman filtering with intermittent observations," *IEEE Trans. Autom. Control*, vol. 49, no. 9, pp. 1453–1464, Sep. 2004.
- [36] Y. Dai, M. Sheng, J. Liu, N. Cheng, X. Shen, and Q. Yang, "Joint mode selection and resource allocation for D2D-enabled NOMA cellular networks," *IEEE Trans. Veh. Technol.*, vol. 68, no. 7, pp. 6721–6733, Jul. 2019.
- [37] M. Sheng, Y. Dai, J. Liu, N. Cheng, X. Shen, and Q. Yang, "Delay-aware computation offloading in NOMA MEC under differentiated uploading delay," *IEEE Trans. Wireless Commun.*, vol. 19, no. 4, pp. 2813–2826, Apr. 2020.
- [38] P. D. Tao *et al.*, "The DC (difference of convex functions) programming and DCA revisited with DC models of real world nonconvex optimization problems," *Ann. Oper. Res.*, vol. 133, nos. 1–4, pp. 23–46, 2005.
- [39] L. Xie, Q. Li, W. Mao, J. Wu, and D. Chen, "Achieving efficiency and fairness for association control in vehicular networks," in *Proc. 17th IEEE Int. Conf. Netw. Protocols*, Princeton, NJ, USA, 2009, pp. 324–333.
- [40] Z. Li, C. Wang, and C.-J. Jiang, "User association for load balancing in vehicular networks: An online reinforcement learning approach," *IEEE Trans. Intell. Transp. Syst.*, vol. 18, no. 8, pp. 2217–2228, Aug. 2017.



Ling Lyu (Member, IEEE) received the B.S. degree in telecommunication engineering from Jinlin University, Changchun, China, in 2013, and the Ph.D. degree in control theory and control engineering from Shanghai Jiao Tong University, Shanghai, China, in 2019.

She joined Dalian Maritime University, Dalian, China, in 2019, where she is currently an Associate Professor with the School of Information Science and Technology. She was a visiting student with the University of Waterloo, Waterloo, ON, Canada, from

September 2017 to September 2018. Her current research interests include wireless sensor and actuator network and application in industrial automation, the joint design of communication and control in industrial cyber-physical systems, estimation and control over lossy wireless networks, machine-type communication-enabled reliable transmission in the fifth-generation network, resource allocation, and energy efficiency.



Yanpeng Dai (Member, IEEE) received the B.Eng. degree from Shandong Normal University, Jinan, China, in 2014, and the Ph.D. degree from Xidian University, Xi'an, China, in 2020.

He is currently an Assistant Professor with the College of Information Science and Technology, Dalian Maritime University, Dalian, China. His research interest includes resource management and interference coordination of heterogeneous wireless networks.



Nan Cheng (Member, IEEE) received the B.E. and M.S. degrees from the Department of Electronics and Information Engineering, Tongji University, Shanghai, China, in 2009 and 2012, respectively, and the Ph.D. degree from the Department of Electrical and Computer Engineering, University of Waterloo, Waterloo, ON, Canada, in 2016.

He worked as a Postdoctoral Fellow with the Department of Electrical and Computer Engineering, University of Toronto, Toronto, ON, Canada, from 2017 to 2019. He is currently a Professor with the State Key Laboratory of ISN and the School of Telecommunication Engineering, Xidian University, Xi'an, China. His current research focuses on 5G/6G, space-air-ground-integrated network, big data in vehicular networks, and self-driving system. His research interests also include performance analysis, MAC, opportunistic communication, and application of AI for vehicular networks.



Shanying Zhu (Member, IEEE) received the B.S. degree in information and computing science from the North China University of Water Resources and Electric Power, Zhengzhou, China, in 2006, the M.S. degree in applied mathematics from the Huazhong University of Science and Technology, Wuhan, China, in 2008, and the Ph.D. degree in control theory and control engineering from Shanghai Jiao Tong University, Shanghai, China, in 2013.

From 2013 to 2015, he was a Research Fellow with the School of Electrical and Electronic Engineering, Nanyang Technological University, Singapore. He joined Shanghai Jiao Tong University in 2015, where he is currently an Associate Professor with the Department of Automation, School of Electronic Information and Electrical Engineering. His research interests focus on multiagent systems and wireless sensor networks, particularly in coordination control of mobile robots and distributed detection, and estimation in sensor networks and their applications in industrial networks.

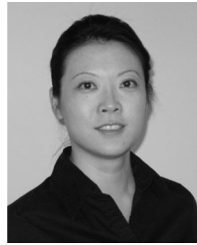


Xinping Guan (Fellow, IEEE) received the B.Sc. degree in mathematics from Harbin Normal University, Harbin, China, in 1986, and the Ph.D. degree in control science and engineering from Harbin Institute of Technology, Harbin, in 1999.

He is currently a Chair Professor with Shanghai Jiao Tong University, Shanghai, China, where he is the Dean of the School of Electronic, Information and Electrical Engineering, and the Director of the Key Laboratory of Systems Control and Information Processing, Ministry of Education of China. Before

that, he was the Executive Director of Office of Research Management, Shanghai Jiao Tong University, and a Full Professor and the Dean of Electrical Engineering, Yanshan University, Qinhuangdao, China. He has authored and/or coauthored five research monographs, more than 200 papers in IEEE transactions and other peer-reviewed journals, and numerous conference papers. His current research interests cover industrial network systems, smart manufacturing, and underwater networks.

Dr. Guan received the Second Prize of the National Natural Science Award of China, in 2008 and 2018, the First Prize of Natural Science Award from the Ministry of Education of China, in 2006 and 2016, and the "IEEE Transactions on Fuzzy Systems Outstanding Paper Award" in 2008. He is a "National Outstanding Youth" honored by NSF of China, "Changjiang Scholar" by the Ministry of Education of China, and "State-Level Scholar" of "New Century Bai Qianwan Talent Program" of China. As a Principal Investigator, he has finished/been working on more than 20 national key projects. He is the Leader of the prestigious Innovative Research Team of the National Natural Science Foundation of China. He is an Executive Committee Member of Chinese Automation Association Council and the Chinese Artificial Intelligence Association Council.



Bin Lin (Member, IEEE) received the B.S. and M.S. degrees from Dalian Maritime University, Dalian, China, in 1999 and 2003, respectively, and the Ph.D. degree from the Broadband Communications Research Group, Department of Electrical and Computer Engineering, University of Waterloo, Waterloo, ON, Canada, in 2009.

She is currently a Full Professor and the Dean of Communication Engineering Department, School of Information Science and Technology, Dalian Maritime University. She also works with the Network Communication Research Center, Peng Cheng Laboratory, Shenzhen, China. She has been a Visiting Scholar with George Washington University, Washington, DC, USA, from 2015 to 2016. Her current research interests include wireless communications, network dimensioning and optimization, resource allocation, artificial intelligence, maritime communication networks, edge/cloud computing, wireless sensor networks, and Internet of Things.

Prof. Lin is an Associate Editor of *IET Communications*.



Xuemin (Sherman) Shen (Fellow, IEEE) received the Ph.D. degree in electrical engineering from Rutgers University, New Brunswick, NJ, USA, in 1990.

He is currently a University Professor with the Department of Electrical and Computer Engineering, University of Waterloo, Waterloo, ON, Canada. His research focuses on network resource management, wireless network security, Internet of Things, 5G and beyond, and vehicular *ad hoc* and sensor networks.

Prof. Shen received the R. A. Fessenden Award in 2019 from IEEE, Canada, the Award of Merit from the Federation of Chinese Canadian Professionals, Ontario, in 2019, the James Evans Avant Garde Award in 2018 from the IEEE Vehicular Technology Society, the Joseph LoCicero Award in 2015, the Education Award in 2017 from the IEEE Communications Society, the Technical Recognition Award from Wireless Communications Technical Committee in 2019, and the AHSN Technical Committee in 2013. He has also received the Excellent Graduate Supervision Award in 2006 from the University of Waterloo and the Premier's Research Excellence Award in 2003 from the Province of Ontario, Canada. He served as the Technical Program Committee Chair/Co-Chair for IEEE Globecom 2016, IEEE Infocom 2014, IEEE VTC 2010 Fall, IEEE Globecom 2007, and the Chair for the IEEE Communications Society Technical Committee on Wireless Communications. He was the elected as the IEEE Communications Society Vice President for Technical and Educational Activities, the Vice President for Publications, the Member-at-Large on the Board of Governors, the Chair of the Distinguished Lecturer Selection Committee, and the Member of IEEE ComSoc Fellow Selection Committee. He was the Editor-in-Chief of the IEEE INTERNET OF THINGS JOURNAL, IEEE NETWORK, and *IET Communications*. He is a registered Professional Engineer of Ontario, Canada, an Engineering Institute of Canada Fellow, a Canadian Academy of Engineering Fellow, a Royal Society of Canada Fellow, a Chinese Academy of Engineering Foreign Member, and a Distinguished Lecturer of the IEEE Vehicular Technology Society and Communications Society.